Photolytic spectroscopy of simple molecules. I. The production of 52 D atoms from Cs2

C. B. Collins, J. A. Anderson, D. Popescu, and Iovitzu Popescu

Citation: The Journal of Chemical Physics **74**, 1053 (1981); doi: 10.1063/1.441238
View online: http://dx.doi.org/10.1063/1.441238
View Table of Contents: http://scitation.aip.org/content/aip/journal/jcp/74/2?ver=pdfcov
Published by the AIP Publishing

Photolytic spectroscopy of simple molecules. I. The production of 5 ^2D atoms from Cs_2

C. B. Collins and J. A. Anderson

Center for Quantum Electronics, The University of Texas at Dallas, Richardson, Texas 75080

D. Popescu and Iovitzu Popescu

Central Institute of Physics, Bucharest/Magurele, Romania
(Received 8 August 1980; accepted 30 September 1980)

A two-photon technique is reported for the measurement of relative cross sections for the selective photolysis of simple molecules into particular product channels. In a demonstration of this method two independently tunable dye lasers were used to sequentially dissociate molecules of Cs_2 for wavelengths in the visible range and then to excite the resulting products to Rydberg states which could be readily ionized for detection. With this system the spectra were determined for the selective photolysis of Cs_2 into product atoms in the $5\,^2D_{3/2}$ and $5\,^2D_{5/2}$ states. Two relatively broad absorption bands were found, each of which led to the preferential population of a different fine structure components of the $5\,^2D$ products. Analysis of the photolysis spectra indicated that both dissociation and predissociation mechanisms were responsible and led to the identification of a new $^1\Sigma_u$ and $^3\Sigma_u$ state correlated with the $5\,^2D$ atomic states.

INTRODUCTION

The recent efforts which have developed in laser chemistry and laser isotope separation have tended to refocus spectroscopic interest upon dissociation processes in molecules. For example, if it is intended to selectively activate an isotopic or reactive species, photodissociation of a parent molecule appears to be a nearly ideal mechanism.

To date the most popular approach to be applied in this type of selective photolysis has been the use of multiphoton excitation and dissociation. For heteronuclear molecules, this has generally been accomplished by illuminating the parent molecule with wavelengths whose quanta were much smaller than the vertical dissociation energy of the ground state. The actual excitation, then, proceeded in a stepwise fashion with the first step usually corresponding to the resonant excitation of a particular vibrational or rotational state which could ultimately lead to the production of a dissociation fragment of the desired type. Thus, to obtain a high degree of selectivity between the products, the illuminating sources had to have extremely narrow bandwidths and precisely controlled wavelengths. The isotopically selective dissociation of SF_6 with CO_2 laser photons has typified this approach and the substantial progress which has been accomplished with that system, as well as with many others, has been summarized recently in an excellent review.[1]

Unfortunately, however, if perceived as reactant species, coherent photons are exceedingly expensive, their cost being elevated further by the degree of precision with which the wavelength must be regulated and by the narrowness of the bandwidth which must be maintained. These factors have tended to impede the practical utilization of the multiphoton schemes for implementing laser chemistry and have provided a clear motivation for the consideration of alternative schemes for selectively exciting reactive species.

It is interesting that it was such an alternative scheme that led to what was apparently the first observation to be reported in the literature[2] of selective photodissociation induced by a laser. In that work the direct dissociation of H_2 was accomplished by the nearly resonant excitation to a repulsive electronic state. The transition was induced by the simultaneous absorption of relatively few photons of a fixed wavelength. Because of the fixed wavelength, spectra were not obtained and the identities of the dissociation products were inferred from the number of photons required to ionize the species at that wavelength, so that the products might be detected.

Spectroscopic identification of the products of molecular dissociation induced by laser radiation was first reported by Collins *et al.*[3] for the dissociation of Cs_2 with the output from a tunable dye laser. As in the work of the Saclay group,[2] it was found that a multiphoton absorption could occur with high probability through a resonant intermediate state that was electronically excited and unstable against dissociation on the time scale of the multiphoton process. The resulting two-photon ionization spectra of Cs_2, showing resonances for the absorption to a dissociative state followed by absorption from an excited state of a product Cs atom, were reported[3] in 1974. These resonances were termed hybrid by the authors and they were subsequently found in Rb,[4] K,[5] In,[6] and Yb.[7] In appearance they took the typical forms of Rydberg series of discrete absorption lines from particular excited states of the dissociation products that were modulated in intensity by the probabilities for the molecular part of the absorption that had led to the dissociation of the parent dimer. In some cases the Rydberg series spectra were observed to be anamolously terminated when wavelengths were reached at which molecular dissociation did not occur. However, the span of wavelengths over which hybrid resonances could be found, even in the first dispersion curves obtained,[3] suggested that selective photolysis could be accomplished over fairly generous bandwidths of excitation, at least for these types of simple molecules.

Because of this promise that molecular photolysis accomplished through electronic excitation might maintain product selectivity over broader bandwidths, it appears

 0021-9606/81/021053-14$01.00

that this alternative scheme might lend itself more readily to the production of practical magnitudes of populations of selected states even with incoherent sources of illumination. If actually realized, such a possibility would greatly increase the probabilities for the development of economically viable processes requiring reactant state selection. Unfortunately, the practical application of such techniques would generally require detailed knowledge of the dissociative state to be excited, of the states of the products with which it is correlated, and of the dynamics of the dissociation process which determine the extent to which the product channels might be mixed by crossings of the potentials describing long range forces. As often employed, the examination of spontaneous fluorescence from the products of laser induced photolysis provides[8] some of this information but it is generally susceptible to uncertainties in the unique identification of the product channels. Exceptions occur in isolated systems in which the fluorescence lifetimes of the dissociation products are much less than the characteristic times for collisional mixing of the states, as was the case in the classical measurement[9] of the various partial cross sections for the photolysis of H_2 and in the measurement of the photolysis of alkali dimers at very low pressures into the lowest excited atomic states.[10]

It was suggested[3] in one of the first reports of laser photolysis through electronically excited states that the envelope contributed to the spectra of hybrid resonances by the molecular part could be isolated and studied as a function of wavelength by using photons from separately tunable lasers. Furthermore, if the lasers were pulsed, operating for a period short compared to the inverse collision frequency of the dissociation products with the components of the absorbing vapor, the diffuse molecular bands which were found could be uniquely correlated with their dissociation products even at the higher vapor pressures needed for greater sensitivity. This suggestion was reiterated in 1976 by Su *et al.*[11] The technique of these proposals was finally realized[12] when the absorption cross section of Cs_2 was recently resolved into its component cross sections for photolysis into particular product channels at wavelengths in the blue region of the spectrum. This particular segment of the spectrum was chosen for the demonstration because prior work[13] had shown the appearance of that part of the classical absorption spectrum to be a smoothly continuous function of wavelengths, suggesting that there would be an abundance of dissociative mechanisms occurring in the states excited at those wavelengths. In the absence of thermal excitation of the parent Cs^2 only four possible products, $6\,^2P_{1/2}$, $6\,^2P_{3/2}$, $5\,^2D_{3/2}$, and $5\,^2D_{5/2}$, conserved energy when the illuminating wavelength was greater than the limit of 460 nm used in that experiment. The relative cross sections for the production of each were determined in an environment which was essentially free from collisions that might have tended to mix the channels for dissociation on the time scale of the experiment. The considerable sensitivity and resolution which were achieved clearly indicated that the multiphoton technique introduced there can be of significant utility to photolytic spectroscopy. Moreover, relatively broadband channels were found for photolysis of Cs_2 that led to distributions of product populations which were selective to an unexpected degree. Those results essentially implied that large populations of selected states of dissociation products could be produced as a result of the illumination of parent molecules with filtered incoherent radiation, at least for the rather specific example chosen.

In the work reported here, this new multiphoton technique for photolytic spectroscopy[12] was used in a more general survey of the absorption spectrum of Cs_2 over the full range of visible wavelength in order to determine the part of the spectrum leading to the production of Cs atoms in $5\,^2D_{3/2}$ and $5\,^2D_{5/2}$ states. As in the preliminary work,[12] the relatively short delay between the creation of the dissociation products and their excitation to detectable levels insured that the states of the products were not mixed by any collisional processes subsequent to the initial dissociation. Thus, direct correlation could be made between the structures in the molecular spectrum that were excited at a given wavelength and the resulting products of dissociation.

Two strong absorption bands separated by about 80 nm were found. Each had a relatively broad width of around 25 nm and each lead to the preferential photolysis of the parent Cs_2 into a different fine structure component of the $5\,^2D$ atomic state. Excitation of the blue band was found to favor dissociation into the $\Omega = \frac{3}{2}$ state by a factor of about 1.8 to 1, while the green band selectively populated the $\Omega = \frac{5}{2}$ component by a factor of 2.8 to 1. This was quite an unexpected result since it implies that the higher energy dissociation product, the $5\,^2D_{5/2}$ can be obtained by photolysis with lesser energy than necessary to select for the low energy product. It is clear that such a result could not have been anticipated from the theoretical potential curves available prior to this work and this attests to the importance of the experimental measurement of these quantities.

Besides being interesting in themselves, the spectra or selective photolysis obtained in this work provided the basis for a better understanding of the potential curves of Cs_2. The analysis of those results in conjunction with the existing literature permitted the identification of two previously unknown molecular states, a $^3\Sigma_u$ state and a $^1\Sigma_u^+$ state, and permitted their correlation with the separated atom limits. The companion paper,[14] immediately following, describes the extension of these techniques to the study of the selective photolysis of Cs_2 leading to the production of $6\,^2P_{3/2}$ and $6\,^2P_{1/2}$ atoms. The results of that work, together with those reported here for the production of 5D-state populations, proved sufficient for the construction of a more comprehensive set of potential curves for Cs_2 as discussed in the following paper. This substantially increased understanding of the structure of Cs_2 seems to attest to promise held by this new multiphoton technique for the detailed characterization of the repulsive states of simple molecules that are becoming of critical interest in a variety of applications.

THEORY

Ideally, the photolysis of a simple molecule can be

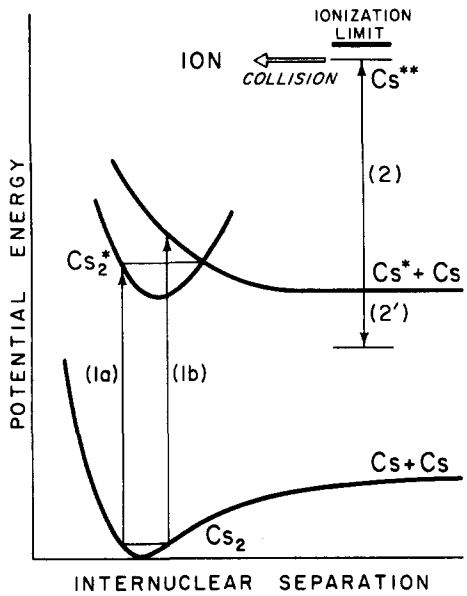

FIG. 1. Schematic representation of the multiphoton process used in this work for studying the selective photolysis of Cs_2. Typical molecular potentials are plotted as functions of internuclear separation with radiative transitions shown by arrows. The first transition causing photolysis is designated (1a) for predissociation or (1b) for direct dissociation. The second transition used to excite the dissociation products Cs* to the readily ionized state Cs** is denoted (2), while (2') shows a possible transition for fluorescent detection.

accomplished by inducing a transition to an electronically excited state which is unstable for one of several possible reasons. A typical situation is shown in Fig. 1 where photolysis could occur through the excitation of a transition, such as (1a), to a bound state which can subsequently predissociate to produce Cs*. The principal restriction is that there must be an intersection at a suitable energy of the potential curve for that bound state with a curve for a repulsive state of the proper symmetry. The excitation of a transition, such as (1b), directly to a repulsive state correlated with the same dissociation limit would comprise an alternative channel for the production of Cs* by the photolysis of Cs_2. In the Born–Oppenheimer approximation, the relative importance of channels (1a) and (1b), together with their dependences upon the wavelength of the source inducing the transition would depend upon the matrix elements for the transition between the electronic states, the Franck–Condon factors depending upon the initial and final states of the nuclear motion, the Honl–London factors describing the probability for any changes in rotational motion, and upon the probabilities for spontaneous dissociation of the excited state formed. In principle, except for the last, these are well-known quantities whose product is the transition probability for that particular absorption band of Cs_2. When multiplied by the last quantity, and with an adjustment of numerical constants it becomes the cross section for the photolysis of Cs_2 into the products Cs* + Cs. It is the measurement of this cross section that lies at the focus of the work reported here.

Unfortunately, in realistic cases the system shown in Fig. 1 is greatly complicated by the occurrence of many additional repulsive and weakly bound states correlated at large internuclear separations with the same dissociation limits. The transitions to these states, if allowed by the appropriate selection rules, are then distributed over a large spread of wavelengths, usually becoming overlapped by transitions to molecular levels correlated with other limits. Because of this, studies by conventional means of transitions to repulsive and dissociative states have usually revealed composite absorption continua which were generally featureless and, thus, which could not lead to the depth of understanding that has been reached with the well-bound states of molecular systems.

For example, to conventional spectroscopy the absorption spectrum of Cs_2 has presented a very complex picture.[13] In the visible region, it contains three main features consisting of broad absorption maxima at 480, 580 and 630 nm. Although the first investigation of these molecular features with high resolution was initiated by Loomis and Kusch[15] in 1934, only the study of the red system has yielded detailed and comprehensive results[16,17] serving to identify that band as belonging to the transition, $C\,^1\Pi_u - X\,^1\Sigma_g^+$. Analyses had been rendered consistently difficult because high resolution spectra had been found to contain a profusion of poorly resolved or unresolved lines as a result of the small vibrational and rotational spacings of the states of Cs_2. In the red band the possible existence of additional underlying continua was masked by this structure. The blue system at 480 nm has become the subject of several recent studies,[18,19] and although a complete understanding has been elusive, it is currently believed to result from the $X\,^1\Sigma_g - E\,^1\Pi_u$ transition. Essentially nothing seems to have been learned about the green system at 580 nm from conventional absorption spectroscopy. Thus, if significant levels of photolysis are to be found for Cs_2, it is most reasonable to expect them to be found contributing to the blue and green bands which have not been satisfactorily identified in terms of transitions between well-bound molecular states. Since there must be 12 molecular states arising from the manifold $Cs + Cs(5\,^2D)$, alone, and since only one, $C\,^1\Pi_u$, has been found to be a bound state, it would not be surprising to find not one, but a number of states to which transition from the ground state of Cs_2 could contribute continua overlapping the known, but unresolved blue and green absorption bands.

Conceptually, a first means of resolving these difficult spectral features would be to separate them into component bands each correlated with different transitions in the separated atom limit. For example, in Fig. 1 the band resulting from transitions such as (1a) or (1b) would be correlated with the transition, $Cs + h\nu \rightarrow Cs^*$, in the limit of separated atoms. While that limiting transition might actually be forbidden by selection rules at large internuclear separations, still the correlation of the upper molecular level with the separated atom limit belonging to the particular state mediating the dissociation provides a useful point of departure for subsequent identification of the actual states involved. It also provides a basis for the study of the nature of the dissociation process. Practically, such a resolution and

correlation would produce the spectrum for the selective photolysis of the ground state molecules into the particular product, Cs*.

In the few studies undertaken previously[8-10] the isolation of particular channels for photolysis was accomplished by experimentally correlating absorption data from transitions such as (1a) and (1b) in Fig. 1 with fluorescence radiation from a transition, such as (2′), emitted by the dissociation products. To be successful such a technique required: (1) that the probability for the emission of the fluorescence be high in comparison to the probability that the state would be quenched nonradiatively, (2) that the emission occur before collisional processes would transfer the excitation from some other product state into Cs* and the reverse, and (3) that a transition such as (2′) be found at a reasonable wavelength for detection. These requirements generally limited the exercise of this technique to systems in environments having low frequencies for the occurrence of collisions violating the second requirement above and, hence, to very low pressures. This, in turn, placed very severe restrictions upon the sensitivity which could be achieved. For example, the photolysis of Cs_2 into $6\,^2P$ product states of Cs* was rendered possible[10] through the detection of the fluorescence from the resonance transition to the ground atomic state. However, photolysis into $5\,^2D$ states apparently was not attempted because of the longer radiative lifetime and because of the unfavorable wavelength for detection, near 3.3 μm.

The multiphoton technique introduced recently[12] overcame these difficulties and demonstrated a very high sensitivity for detection. In that system, the products of dissociation were detected through the absorption of a second photon in a transition such as (2) in Fig. 1. However, instead of attempting to detect the slight attenuation of an illuminating beam of wavelength corresponding to transition (2), the strategy of using the second transition to populate a relatively long-lived Rydberg state, Cs**, was employed. Then, as had been demonstrated in much earlier work,[20] if that Cs** state were sufficiently close in energy to the ionization limit, it would have essentially unit probability for undergoing collisional ionization, either to Cs_2^+ or to $Cs^+ + Cs^-$, through associative ionization as a first step, or to Cs^+ by simple inelastic collisions with the majority species in the medium. The resulting ionization was then detected in comparison to a background ionization which tended to be intrinsically low.

In any more general application of these multiphoton techniques for the investigation of molecular photolysis the occurrence of significant levels of background ionization must be considered. Since a straightforward use of chopped illumination or pulsed lasers, and phase sensitive detection will eliminate background ionization unrelated to all absorption processes, only competing channels for photoionization can present material difficulties. Those must either be controlled during the experiment or removed during the subsequent analysis.

It is important, then, to consider what other multiphoton channels may contribute to the ionization signal so that an optimized experimental procedure may be identified. Figure 2 shows a schematic representation of the most likely paths and excited state intermediaries which could be involved in multiphoton ionization of cesium vapor. It is useful in considering these processes to assume a fixed temporal dispersion between the pulses of radiation at the two different wavelengths used to illuminate the vapor. In the idealized representation shown in Fig. 1, the first pulse had been of a wavelength suitable to excite transitions denoted (1a) or (1b) while the second pulse had been delayed to permit time for the dissociation process. Of course, the latter pulse had been assumed to contain wavelengths suitable for the excitation of the dissociation product, Cs*, to the Rydberg state, Cs**. The same essential concepts were incorporated in the representation of the more general scheme shown in Fig. 2, where all transitions which could be possibly excited by the first pulse are shown by unbroken arrows and those possibly excited by the delayed pulse are shown by the broken arrows. While it is intended that the first pulse dissociate the molecule and the second excite the products, many other undesirable combinations are possible if the wavelengths involved are accidentally resonant with transitions between other states which may be appreciably populated.

The desired channel for ionization which had been isolated in Fig. 1 is identified in Fig. 2 by the heavy arrows representing transitions between the intermediate species shown as boxes with heavy boundaries. Nonradiative steps have been shown as the open arrows. Alternative channels for photoionization can be seen to involve singly and doubly primed species which may or may not be identical to the unprimed species. For example, the first step in the central channel involves either the absorption by Cs_2 of a photon from the first laser pulse to produce the excited state Cs_2^* or of a photon from the second laser pulse to produce $Cs_2^{*\prime}$. Most generally the two pulses will contain completely different wavelengths so it is likely that $Cs_2^{*\prime}$ will be a state other than Cs_2^*. However, this is not necessarily so, as the absorption band of the transition to Cs_2^* may span a range of wavelengths sufficient to include those of both pulses. In a sense the two alternatives ultimately produce different components of the resulting ion population. The leftmost branch of the central channel will produce a component of population which should depend linearly upon the intensities of both laser pulses, while the population component resulting from excitation of the rightmost branch should have no dependence upon the intensity of the first laser pulse, provided saturation effects are avoided. The two components of ion population produced by these branches in the central channel have been designated together with the unprimed and primed intermediate state populations as one and two, respectively, as shown. They can be experimentally resolved by varying the intensity of the first laser pulse.

To facilitate the consideration of the different ionization channels it is useful to alphabetically index them so that the central channel becomes b, as shown in Fig. 2, with the two distinguishable subpopulation of ions becoming b_1 and b_2. Then, as can be seen population a will be produced by processes in which the initial transition is the same as in the central b_1 channel. How-

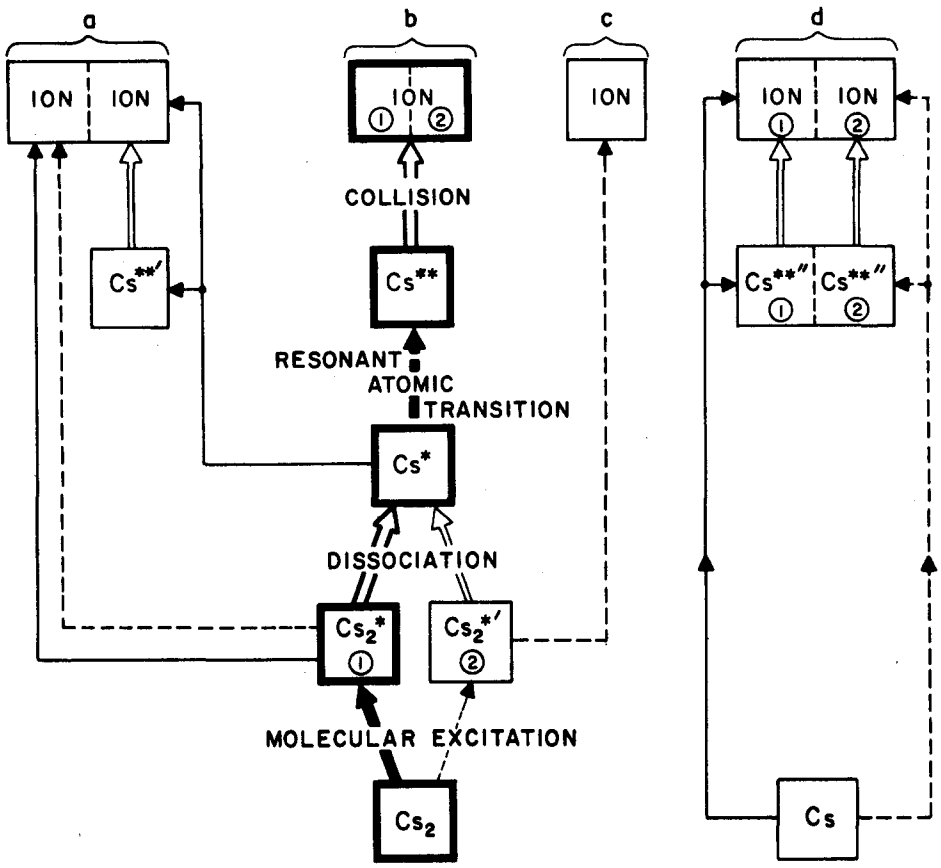

FIG. 2. Schematic representation of the absorption transitions and kinetic steps involved in the multiphoton process employed in this study of selective photolysis. Competing processes contributing to background experimental yield have also been shown. Heavy lines identify the reaction path of interest. Solid and broken arrows indicate, respectively, transitions excited by absorption from either the initial pulse of wavelength λ_1 or from the delayed pulse of wavelength λ_2. Indicated by braces are groupings of reaction paths which facilitate data reduction as explained in the text.

ever, either the Cs_2^* must be directly photoionized by the absorption of the second photon from either laser pulse before dissociation, or the Cs* can be directly photoionized by the absorption of a second photon from the first laser pulse if the dissociation occurs rapidly enough. As reported previously,[21] the absorption of the second photon at visible wavelengths prior to dissociation will lead directly to ionization as shown in Fig. 2. Conversely, however, after dissociation the ionization threshold may be great enough that photoionization cannot be accomplished by the absorption of a second photon at the longer visible wavelengths. The representation of that particular component of channel *a* in Fig. 2 reflects this limitation by showing a branch point at which the absorption of a second photon leads either to the population of a Rydberg state Cs**' or directly to photoionization. Population *c* is another example of two photon transitions through molecular intermediate states,[21] as mentioned above, while population *d* is the result of the corresponding absorption by Cs of two photons from either the first or second pulses.[22] Depending upon photon energies in the latter channel either an intermediate Rydberg state Cs**'' or direct photoionization may be produced.

In this work the separation of signal b_1 resulting from the selective photolysis channel under study from the hybrid resonance signal b_2, as well as from the other background signals, depended upon two assumptions. First it was assumed that intensities were low enough to avoid problems of saturation of the transitions and depletions of the populations. Second it was assumed that only populations b_1, b_2, and d depended critically upon the precise value of the wavelength of the second laser pulse λ_2. As shown in Fig. 2, this required that population c depend upon λ_2 only through a continuous transition such as might be expected from $Cs_2^{*'} \rightarrow Cs_2^+$, or that any structure in that transition be clearly resolvable from the atomic line resulting from the transition Cs* → Cs**.

From Fig. 2 it can be seen, in principle, that population b_1 can be isolated in two steps. Because only population b should show a strong resonance peak at the wavelength λ_2 (Cs* → Cs**) corresponding to the excitation of the transition from product states Cs* to Rydberg state Cs**, its magnitude could be determined by tuning the wavelength of the delayed laser pulse while holding the wavelength of the first pulsed fixed. Then, the component due to b_1 could be obtained by exploiting the fact that the other component should not depend upon the intensity of the first pulse. The desired procedure for isolating the b_1 component can be quantitively expressed by letting the ion signal resulting from illumination of the vapor with an intensity $I_1(\lambda)$ at the first wavelength and subsequently with $I_2(\lambda)$ at the second by $S[I_1(\lambda), I_2(\lambda)]$. For these purposes it is only necessary to distinguish between wavelengths λ_R for the second pulse that correspond to the resonant excitation of the product transition Cs* → Cs**, and other nonresonant wavelength, λ_{NR}. Then from Fig. 2 it can be seen that

$$S[I_1, I_2(\lambda_R)] = a + b_1 + b_2 + c + d_1 + d_2 , \quad (1)$$

while

$$S[I_1, I_2(\lambda_{NR})] = a + c + d_1 + d_2 . \quad (2)$$

Subsequently, blocking the first pulse would eliminate all channels involving a solid arrow in Fig. 2 giving

$$S[0, I_2(\lambda_R)] = b_2 + c + d_2 , \tag{3}$$

while off-resonance,

$$S[0, I_2(\lambda_{NR})] = c + d_2 . \tag{4}$$

Channel d_2 is included as a nonresonant process because the transition $Cs \rightarrow Cs^{**\prime\prime}$ might represent the nonresonant absorption of two photons to create a virtual state subsequently ionized during its lifetime by collisions or by a third photon. Combining Eqs. (1), (2), (3), and (4) gives

$$b_1 = S[I_1, I_2(\lambda_R)] - S[I_1, I_2(\lambda_{NR})] - \{S[0, I_2(\lambda_R)] - S[0, I_2(\lambda_{NR})]\} , \tag{5}$$

the desired expression for the component describing the selective photolysis in terms of populations of ions which can be experimentally resolved.

Elementary considerations are sufficient to express the ionization signal b_1, obtained experimentally as shown in Eq. (5), in terms of molecular parameters. In the linear region of intensities the yield of product population $[Cs^*]$ at the position q in the absorbing vapor is given at the end of the photolysis pulse by

$$[Cs^*(q)] = \sigma_{Cs^*}(\lambda_1)[Cs_2](\hbar\omega_1)^{-1}\int I_1(\lambda_1, q)\, dt , \tag{6}$$

where $\sigma_{Cs^*}(\lambda_1)$ is the cross section for the photolytic production of Cs* at the wavelength λ_1 of the first laser pulse, $(\hbar\omega_1)$ is the corresponding energy of a photon, $I_1(\lambda_1, q)$ is the part of the time-dependent intensity of the initial laser pulse lying within the absorption bandwidth at the spatial position q, and brackets denote concentrations. Assuming the inverse destruction frequency of Cs* to be long in comparison to the interpulse time, a similar expression can be obtained for the density of Rydberg atoms Cs** produced by the delayed laser pulse,

$$[Cs^{**}(q)] = \sigma_{Cs^{**}}(\lambda_2)[Cs^*](\hbar\omega_2)^{-1}\int I_2(\lambda_2, q)\, dt , \tag{7}$$

where the terms are the analogs of those appearing in Eq. (6) and where transport has also been assumed to be negligible during the interpulse time. If the probability for the collisional ionization of the Rydberg atoms in state Cs** is denoted by P_A^{**}, the ionization signal b_1, appearing in Eq. (5) that is contributed by the composite process involving the photolytic production of Cs* atoms can be written

$$b_1/(E_1/\hbar\omega_1)(E_2/\hbar\omega_2) = G[Cs_2]\int f_1(q) f_2(q)\, dq\, \{P_A^{**}\sigma_A^{**}(\lambda_2)\}\sigma_{Cs^*}(\lambda_1) , \tag{8}$$

where the integral is taken over the sensitive region of the vapor, and where the substitution

$$\int I_n(\lambda_n, q)\, dt = E_n f_n(q) \tag{9}$$

has been introduced. In this expression E_n represents the energy within the absorption bandwidth of the nth laser pulse, where $f_n(q)$ is the normalized spatial distribution of the laser pulse energy, and G represents the sensitivity and gain of the ionization detector.

In the work reported here, the use of Eq. (8) to obtain values for the cross sections $\sigma_{5D}(\lambda_1)$ for selective photolysis of Cs_2 was facilitated by the particular choices of Cs** and λ_2. The quantities appearing on the left side of Eq. (8) were directly measured at different wavelengths for photolysis while the integral describing the beam overlap was maintained as an experimental invariant. Since the remaining factors on the right, except for the cross section itself, were independent of the photolysis wavelength, values for the relative cross sections for photolysis at different wavelengths to produce a single product were simply proportional to the left-hand side of Eq. (8), evaluated as a function of λ_1. To obtain the relative cross sections for photolysis into different fine-structure components of the product state required only supplementary information about the term in braces. The second factor is essentially the transition probability for the atomic absorption line, Cs* $\rightarrow$ Cs**, and can be obtained readily from the literature.[23] The importance of the first factor has been indicated[24] to depend primarily upon n^{**}, the principle quantum number of the Rydberg state Cs**, and it has been shown[20] for large n^{**} that $P_{Cs^{**}} \sim 1$ for P and D states. Therefore, for excitation to a highly excited Rydberg state for subsequent detection, the term in braces should depend upon n^{**} and L^{**} in $L \cdot S$ coupling through the transition probability, but not upon J^{**}. In that case the relative cross sections for photolysis into different fine-structure components of a particular state of the dissociation products, should be simply proportional to the experimentally measured quantities on the left of Eq. (8), provided n^{**} is the same for both components. The precise values for the terms in braces becomes necessary only in the event of the measurement of photolysis cross sections leading to product states having differing n^* or L^* values. In cases such as those considered in the subsequent companion article, the experimentally measured quantities must be divided by the term in braces.

EXPERIMENTAL METHOD

The experimental scheme used in this work is shown in Fig. 3. As can be seen, two independently tunable, pulsed dye lasers were used to provide, first, the photolysis pulse and, subsequently, the pulse of illumination needed to excite the dissociation products to readily ionized Rydberg states. The dye lasers were pumped by a single nitrogen laser operating at a power level of 300 kW in a 10 nsec pulse. The output from the pump laser was geometrically split into two portions that were separately focused onto the two dye lasers. The output beams from the dye lasers were aligned to be spatially collinear, but were temporally dispersed so that the one used to dissociate the population of parent molecules arrived first at the absorption cell by about the duration of the pulse. An optical delay line was available for the adjustment of the temporal separation of the pulses but the results were not found to be particularly sensitive to this variable unless the order of the occurrence of the

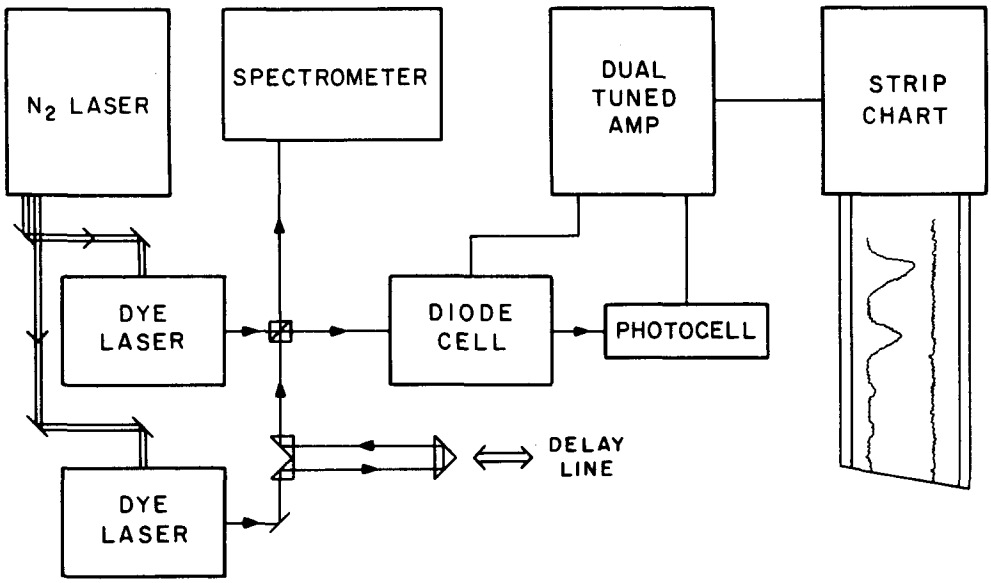

FIG. 3. Schematic representation of the experimental apparatus.

pulses was reversed. As expected, with the reversed temporal sequence the signal from the photolysis channel was completely absent.

The linewidths of the outputs from the dye lasers were of the order of 0.01 nm as determined with a Fabry–Perot etalon and corresponded in magnitude approximately to the resolution with which the wavelength could be set. The full output intensities generally exceeded the limits for linear excitation of the channel for the photolysis and detection of the dissociation products of Cs_2 under the conditions of this experiment. This generally necessitated the adjustment of beam diameters, as well as independent attenuation of the two outputs with neutral density filters until linear operation of the system was obtained. In practice this was verified by measuring the ionization signals developed from the excitation of transitions known[3,20–22] to have linear or quadratic dependences upon the intensity of each laser when used singly to illuminate the vapor. Typically, each laser output was attenuated to deliver peak powers of approximately 12 W to the absorption sample, resulting in experimental intensities on the order of 1.5 kW/cm^2. The excitation sequence was repeated at a rate of about 8 Hz to match the central frequency of the tuned amplifier used to record the signal developed from the resulting ionization. Wavelengths of the laser outputs were determined with a 0.75 m monochromator having a reproducibility of better than 0.1 nm. The intensities of each laser output were monitored with a selenium solar cell used in a ballistic mode and calibrated with a vacuum photodiode. Considerable effort was expended in avoiding effects of local saturation and nonuniformity of the detector surface. The laser intensities were periodically monitored, both totally and individually by alternately blocking and unblocking the two beams in order to obtain the values appearing in the denominator on the left of Eq. (8).

It should be noted in Fig. 3 that the intensity measurements were conducted behind the experimental sample as a matter of convenience. This was possible because the absorption due to the cesium vapor at these densities was considerably less than 1% across the entire visible wavelength range studied 455 to 605 nm, with the exception of the two atomic lines, $6\,^2S_{1/2} - 7\,^2P_{1/2,3/2}$, at 459.3 and 455.5 nm, respectively.

The actual detection of the ionization produced in the photolysis channel was accomplished by including an *in situ* thermionic ion detector in the vapor cell. The particular arrangement is shown schematically in Fig. 4. The detector itself is a modernization of the "Kingdon cage" introduced[25] in 1923 and subsequently used in very

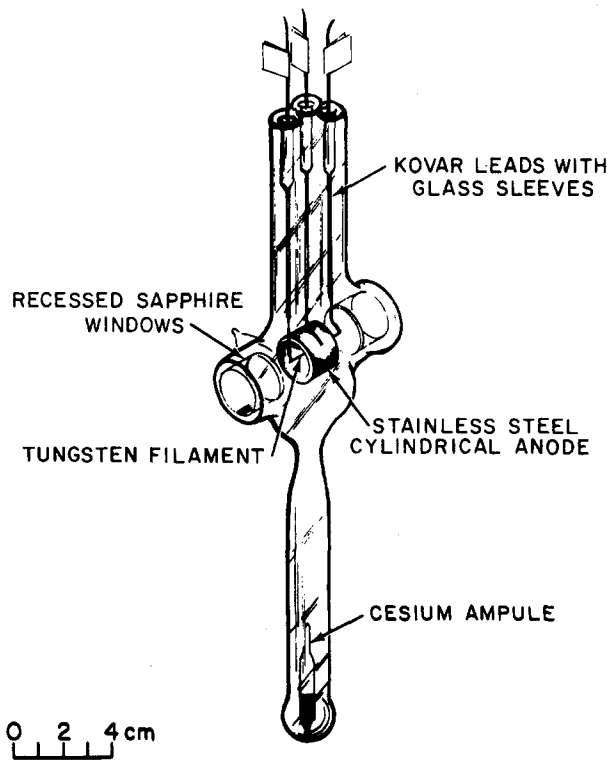

FIG. 4. Absorption cell used in this work, showing details of the thermionic diode employed to detect photoionization.

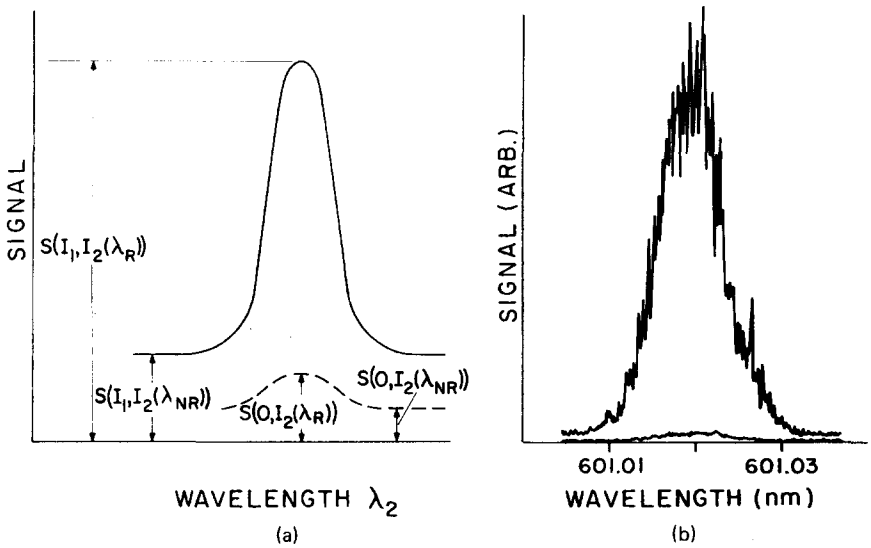

FIG. 5. Dispersion curves as functions of the wavelengths of the delayed laser pulse for the ionization of the particular product state Cs* ($5\,^2D_{5/2}$). The enhancement resulting from photolysis of Cs_2 induced by a preceding pulse of wavelength, 555 nm, is shown by the upper curve of each pair. (a) Schematic representation of typical data serving to identify the nomenclature for the various elements of the data used in separating the desired reaction channel shown in Fig. 2 from background sources of signal. (b) Typical data showing the ionization resonance resulting from the transition step, $5\,^2D_{5/2} \rightarrow 25\,^2F$, in the desired reaction channel. The magnitude of the enhancement resulting from photolytically populating the $5\,^2D_{5/2}$ state can be seen in comparison with noise and background.

early investigations[26–28] of photoionization in cesium vapor. More recently the technique has been revived by Popescu *et al.*[29] making possible many extensions of classical atomic and molecular spectroscopy to alkali transitions of extremely low probability.[3,4,20–22,30,31] Essentially the thermionic ion detector shown in Fig. 4, uses the ionization in the vapor as a distributed grid to control a space-charge limited current flowing between a cathode and an anode arranged to contain the absorbing vapor between them. Under normal conditions, the current through such a thermionic diode is limited because the electrons in transit between cathode and anode cancel the electric field acting on electrons just leaving the cathode.[32,33] This situation holds until the current becomes space-charge limited, finally reaching an upper bound determined by the cathode temperature and corresponding to the maximum rate at which the hot cathode can emit electrons. The dependence of the saturation value on the potential difference across the tube is closely approximated by the Child–Langmuir law. As used in these experiments, the space-charge limited region contained the absorbing vapor under study. While it is not surprising that small densities of neutral atoms and molecules do not significantly affect the behavior of the diode, it has been recently shown[34] that even densities as great as 1 amagat can be tolerated in the system to be described. When ions are introduced into the interelectrode region, they partially cancel the effect of the space-charge electrons and allow an increased current to flow through the tube. The increase in current will persist until the ions are removed from the region, which can occur by neutralization of the ions at the cathode, by diffusion, by recombination of the ions with the space-charge electrons, or by collisional processes involving the neutral populations. Because the ions are much more massive and hence slower moving than the electrons, the time τ_i that an ion remains in the interelectrode region is usually much longer than the transit time τ_e required for an electron to pass from cathode to anode. Since one singly charged ion will at any instant neutralize the effect of one space-charge electron, the net additional charge which will flow through the diode due to the presence of an ion is $e\tau_i/\tau_e$, where e is the charge of an electron. Values of the gain, given by τ_i/τ_e, on the order of 10^4 to 10^6 can easily be realized. As a result of the multitude of processes determining the effective ion lifetime τ_i, the gain of the detector is a complex and sensitive function of its operating conditions. Among the factors influencing the gain are the density and temperature of the absorbing vapor, the temperature and surface conditions of the filament, the potential difference applied to the tube, and the presence of impurity gases.

A critical aspect of the type of experiment described here is that the transitions to the Rydberg states can be detected by observing ions subsequently formed in collisions which involve the excited atoms. The mechanisms responsible for this phenomenon in cesium vapor were originally studied by Mohler and Boeckner,[28] and more recently have been studied in detail by Lee and Mahan.[35] There are three principal processes by which the ions may be formed. One of these, simple thermal ionization of an atom excited to within kT of its ionization limit, is of little importance in the present work. The other two processes both involve ionization via collisional molecular states, but they differ in the type of ion produced. These processes are[29,35]

$$Cs^{**} + Cs \rightarrow Cs_2^{**} \rightarrow Cs_2^+ + e^-, \tag{10}$$

and

$$Cs^{**} + Cs \rightarrow Cs_2^{**} \rightarrow Cs^+ + Cs^- . \quad (11)$$

Using mobility measurements, Lee and Mahan determined that for excited $Cs(n^2P)$ atoms Reaction (10) dominates for principal quantum number $n < 16$ and Reaction (11) dominated for $n > 16$. Since ionization peaks associated with transitions to states for which Reaction (11) should predominate are easily observed[3,20] it is clear that the negative ion is quickly neutralized by photodetachment or some other process,[36] leaving the positively charged ion. The probability that one of the ionizing Reactions (10) or (11) will occur rather than nonionizing relaxation of the atom was deduced by Popescu *et al.*[20] for cesium vapor at pressures appropriate to ion detection with termionic diodes. They found that ionization will occur with essentially unit probability for $Cs(n^2P)$ atoms with $n \geq 28$ and for $Cs(n^2D)$ atoms with $n \geq 15$. Some change in the effective gain of the diode may occur if the identities of the ions change from being predominately molecular to being predominately atomic, but there is evidence that this is not a large effect.[37] In this work, transitions to a limited range of atomic states were considered, and the variation of detector gain due to changes in the ion identities was neglected.

As shown in Fig. 4, the cell used to contain the vapor and *in situ* detector was made of Pyrex 7052 glass and had sapphire optical windows. The cesium reservoir was in a small appendage to the main cell so that the temperatures of the cell and the reservoir could be separately regulated with an appropriate two chamber oven. This allowed independent control of both the temperature and the density of the absorbing vapor. The electrode assembly consisted of a cylindrical stainless steel anode, about 1 cm long × 1 cm diam, and a coaxial filament of 0.15 mm diam tungsten wire. The alignment of the electrodes allowed light to enter the cell through one window, travel through the assembly while remaining parallel to the filament, and exit through the second window giving a total absorption path in the cell of about 3 cm.

RESULTS AND ANALYSIS

All data obtained in this work were taken with a vapor temperature of 250 °C and a saturation temperature for the reservoir of 210 °C. These corresponded to a Cs concentration of 2.14×10^{15} cm^{-3} and a Cs_2 concentration of 7.7×10^{11} cm^{-3}. Calculations of these densities were based on the Taylor–Langmuir formula for the vapor pressure of cesium[38] and on an equilibrium constant deduced from the spectroscopic constants obtained by Kusch and Hessel.[16] Because a tungsten surface maintained at temperatures above about 920 °C will ionize every cesium atom which strikes it,[38,40] it was necessary to operate the tungsten filament in the cesium filled ion detector at less than this temperature. This in turn led to an unacceptably low saturation current for the diode, and steps had to be taken to increase the electron emissivity of the filament surface. As in past work with this type of detector, this was accomplished by coating the filament during assembly with oxides which subsequently reacted with the cesium vapor to form a composite Cs–O–W emitting surface.[41,42] Such surfaces were found to have an electron emissivity many orders of magnitude greater than those of tungsten or tungsten–cesium surfaces.

In operation, the wavelength of the photolysis pulse from the laser was set to successive values which were uniformly spaced across the spectral region studied. Then, for each value of λ_1 the wavelength of the delayed pulse was tuned across a small interval containing the selected atomic transition used to detect a particular dissociation product. Immediately before and after each scan of λ_2 across the atomic line, the pulse energies of the lasers were determined by blocking each in order to permit only one at a time to illuminate the detector. Then, in order to obtain all of the signals required in the analysis defined by Eq. (5), the same wavelength range for the delayed pulse was scanned again with the photolysis beam blocked. An average experimental trial consisted of repetitions of this cycle of measurement while the wavelength of the photolysis pulse was advanced by increments of 2.5 nm. A span of about 25.0 nm could be accommodated in a single trial.

In general, considerable attention was paid to meeting the conditions assumed in the previous theoretical development. As noted above, the cesium vapor was optically thin at the temperatures employed in the experiment. The excitation sequence lasted about 6 nsec, which was short compared to the radiative lifetime[43] of about 1 μsec and mean collision time, also of about 1 μsec, for a $Cs(5^2D)$ atom in the absorption cell. As expected under such conditions, the signal was not observed to be particularly sensitive on this nanosecond scale to the amount of delay introduced between the photolysis pulse and the detecting pulse. Of course, if the order of occurrence of the two pulses were reversed, the signal from channel b_1 in Fig. 2 was found to be completely absent.

As mentioned in the preceding section, low laser powers and large beam cross sections were used to avoid saturation of the radiative transitions. As shown in Fig. 2 any ionization process observed in this experiment required the absorption of two photons so that if no radiative transitions were saturated, the total ion signal observed on-resonance should therefore have depended quadratically on the net energy of the laser pulses incident on the absorption cell. This criterion was verified during the course of each trial by inserting neutral density filters at appropriate positions in the beams. If quadratic signal dependence was not observed, the beams were further attenuated to obtain the desired response. It was also found to be necessary to verify the collinearity of the two laser beams in the absorption cell whenever the photolysis wavelength was changed. Minor realignment of the beams was necessary about 5% to 10% of the time.

Typical data are shown in Fig. 5. In the rightmost panel, the signals resulting from the detection of the ionization produced in the cesium vapor are shown as functions of the wavelength of the delayed laser pulse for the narrow tuning range containing the atomic line resulting from the transition, $5\,^5D_{5/2} \rightarrow 25\,^2F$. The larger curve plots the raw data obtained when the vapor was

illuminated by a preceding pulse tuned to 555 nm, while the smaller resonance shows the signal obtained with the beam from the first laser blocked. The latter signal corresponds to the hybrid resonance reported at this wavelength previously.[3] It results from the photolysis sequence described by channel b_2 in Fig. 2.

The leftmost panel of Fig. 5, shows a schematic reproduction of the type of data reproduced to the right. It serves to identify the various component signals needed for the analysis indicated in Eq. (5). It, however, corresponds to a less favorable case in terms of the ratio of the signal obtained to the background. Usually, the relatively narrow bandwidth of the absorption channel for the detection of the products of photolysis insured that the number of Cs_2^+ ions resulting from the associative ionization of the Rydberg atoms exceeded by 1.5 to 2 orders of magnitude the amount of ionization produced by any of the competing processes such as the direct photoionization of the excited states of Cs_2^* remaining from the excitation produced by the first laser pulse. It was generally found that the composite effect of all of the spurious channels shown in Fig. 2 led to the production of ionization that tended to contribute background signal and noise to the hybrid multiphoton process. The background usually represented less than 20% of the total signal and, thus, could be readily subtracted during the implementation of the analysis scheme of Eq. (5) without degrading the signal to noise ratio. In this sense the schematic representation shown to the left of Fig. 5 corresponded to a worst case for signal-to-background ratio. The actual data shown in the figure represented a more typical situation, and the ultimate limit on sensitivity was generally imposed by a loss of both signals, rather than the loss of a measurable peak.

In the work reported here, the photolysis channels for the production of $5\,^2D_{3/2}$ and $5\,^2D_{5/2}$ atoms were isolated by adjusting the wavelength ranges over which the delayed pulses were scanned to include the transitions to the Rydberg states $20\,^2F_{5/2}$ and $20\,^2F_{5/2,7/2}$, respectively. As discussed above in the section on theory, each of the component steps in the sequence leading to the ionization of the dissociation products should have depended in $L \cdot S$ coupling upon quantum numbers, n and L, but not J. As a consequence, the overall detection efficiency should have been the same for populations in states differing only in J, while having been different from the efficiencies for the detection of products in states having other values of n or L. Thus, as shown in Eq. (8), the relative cross sections for the photolysis of Cs_2 into $5\,^2D_{3/2}$ and $5\,^2D_{5/2}$ states were obtained by simply dividing the bilinear ionization signals, isolated through the application of Eq. (5), by the product of the experimentally measured laser pulse energies.

A fortuitously close coincidence in wavelength between the two atomic transitions $5\,^2D_{3/2} \rightarrow 20\,^2F_{5/2}$ at 601.08 nm and $5\,^2D_{5/2} \rightarrow 25\,^2F_{5/2,7/2}$ at 601.02 nm provided the opportunity to double the rate of data collection. The transitions were sufficiently close that a single scan of λ_2 containing signals for the detection of both $5\,^2D_{3/2}$ and $5\,^2D_{5/2}$ could be made in a reasonable time. For these cases the analyses were rendered somewhat more difficult, but not intractably so. The term in braces in Eq. (8) could no longer be supposed the same for the detection of the two components of the $5\,^2D$ population because of the differing principal quantum numbers of the Rydberg states to which they were excited. Both $n^{**} = 20$ and 25 were sufficiently large that $P_{Cs^{**}}$ could be assumed to be unity in Eq. (8) for both components, but the values of $\sigma_{Cs^{**}}$ were clearly different. However, to a good degree of approximation[20,23] the probabilities for transitions in atomic cesium of the type $5\,^2D \rightarrow n\,^2F$, are proportional to n^{-3}. If the ionization data actually obtained upon excitation of the more convenient transition to $25\,^2F_{5/2,7/2}$ were multiplied by the factor $(25/20)^3$ to correct for this variation of the term appearing in braces in Eq. (8), the results could not be distinguished from the data obtained upon excitation of the transition to $20\,^2F_{5/2,7/2}$. Measurements of both types were used in the construction of the data base described below.

The total data set obtained in this work comprised 1054 observations which were made in 54 trials that covered overlapping ranges of wavelength which together spanned the visible spectra from 457.5 to 605.0 nm. However, variations of the operating conditions of the apparatus between trials caused the terms preceding the braces in Eq. (8) to vary to an extent that it prevented a straightforward comparison of the results of different trials. Rather, the results of each trial had to be multiplied by a factor characteristic of that trial. This compensation was accomplished by a reiterative statistical scheme which multiplied the measurements made in a single trial by a single number, subsequently adjusted to minimize the total variance between all of the measurements of that trial and all of the measurements at comparable wavelengths averaged over other trials. While several different statistical procedures could have been reasonably utilized, the one employed was satisfactorily convergent, yielding an averaged spectrum which was independent of the order in which the trials were considered.

In obtaining the scaling factors for each trial, data from only one of the product channels, $5\,^2D_{3/2}$, was used. The same factors were then used to adjust both channels, so that the relative magnitudes of the signals resulting from each product were preserved. Over the entire range of trials examined, scale factors appeared to vary randomly reaching a value of four in the worst case.

The resulting cross sections for the photolysis of Cs_2 into atoms in the $5\,^2D_{3/2}$ and $5\,^2D_{5/2}$ states are shown in Fig. 6. Because the measurements were made on a constant mesh of 2.5 nm in wavelength, the effective resolution in energy varies from about 70 cm^{-1} at the low wavenumber end of the graph to about 120 cm^{-1} at the other end. Representative error bars at the peaks near 21 000 cm^{-1} show limits of ± 1 standard deviation of the mean. Error limits for other transition energies were found to be scaled to this value in a manner roughly proportional to the measured value of the cross section. The two vertical lines shown in the figure plot computed transition energies from the bottom of the $X\,^1\Sigma_g^+$ ground

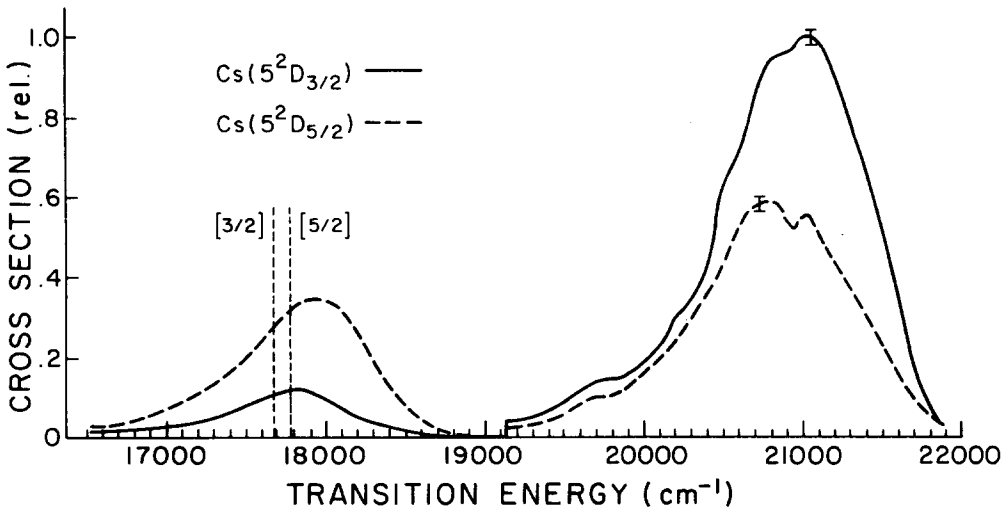

FIG. 6. Relative cross sections as functions of transition energies for the selective photolysis of Cs_2 into the products indicates. Solid and dashed curves identify data for $5\,^2D_{3/2}$ and $5\,^2D_{5/2}$ product states, respectively. The transition energies from the minimum of the Cs_2 potential well to the separated atom limits for each of the two states is indicated by the dashed vertical lines.

state of Cs_2 to the separated atom limits for states involving the two dissociation products. A dissociation energy for the ground state of $D_e = 3197$ cm^{-1} was used to calculate those limits.

As can be seen in Fig. 6, both photolysis spectra show broad bands near 18 000 and 21 000 cm^{-1}. Most surprisingly, the relative cross sections for the two products differ markedly with the production of the higher energy fragment predominating at lower transition energy. The inverse case can also be seen with the lower energy product being preferentially selected by higher transition energy. The crossover appears to occur at the sharp edge observed near 19 100 cm^{-1}.

The branching ratio between the two fine-structure components was obtained as a function of wave number by taking the point by point ratio of the two curves of Fig. 6. The resulting ratio is plotted in Fig. 7 and shows a considerable variation in value between the two bands.

DISCUSSION

A comparison of the results of this experiment with the classical absorption spectrum[13] of Cs_2 shows the photolysis bands of Fig. 6 to be quite similar in appearance to the blue and green systems appearing in conventional spectra. Even the sharp edge near 19 100 cm^{-1} has been found in the classical spectrum and interpreted[15] as being the result of a minimum in the vertical transition energy between the potential energy curves of the ground and upper electronic states.

Upon closer examination, however, it is seen that the lower energy band corresponds only to the shorter wavelength portion of the conventional green band. The portions of that photolysis band at the longer wavelengths appear to be exponentially decreasing with decreasing transition energy from the maxima near the energies corresponding to vertical transitions to the separated atom limits. This immediately suggests that the yellow bands observed in this work might have resulted from transitions directly to states at energies above their dissociation limits and that the photolysis detected at transition energies below the threshold for excitation from the potential energy minimum of the ground state to the separated atom limits was observed only for the component of the Cs_2 population thermally excited prior to the absorption event. The consequent dependence upon the amount of thermal excitation required to conserve energy during the transition would account for the exponential decrease in the photolysis cross section seen in Fig. 6. Even the maxima in the two curves are displaced by reasonable amounts from the separated atom limits with the peak of the green band leading to the production of 5D atoms lying at the higher transition energy than the peak for the production of the $5D_{3/2}$ atoms.

Unfortunately, such a convenient explanation is rendered untenable when the more detailed correlation of

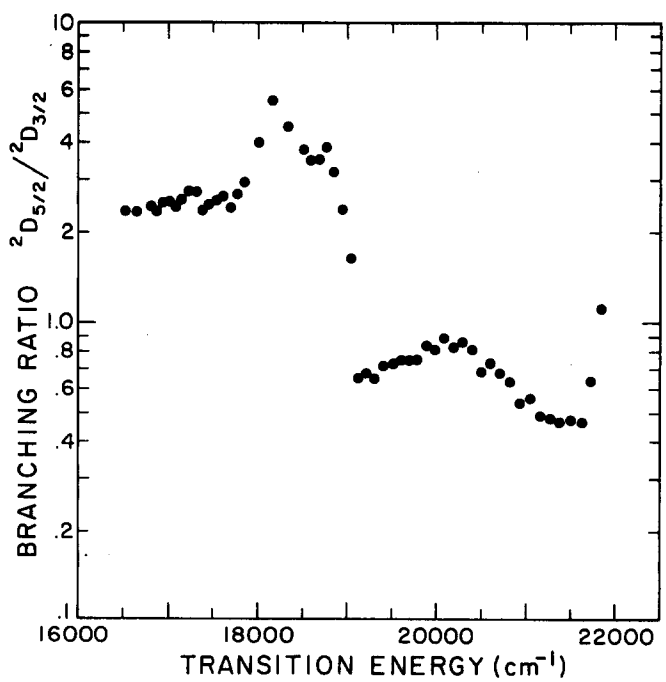

FIG. 7. Branching ratios between the fine structure components of the $5\,^2D$ product states resulting from the photolysis of Cs_2 at the transition energies shown.

the dissociating states with their separated atom limits is attempted. Since the ground electronic state of Cs_2 is $^1\Sigma_g$, only photolysis through states of u symmetry need be considered. From the combination $Cs(5\,^2D) + Cs$, the states $^1\Sigma_u$, $^3\Sigma_u$, $^1\Pi_u$, $^3\Pi_u$, $^1\Delta_u$, and $^3\Delta_u$ can be formed with the proper symmetry. Of these, only the $^1\Pi_u$ has been definitely identified with a classical absorption band, in this case the $X \rightarrow C$ transition near 625 nm. The only other state to which a transition from the ground state would be allowed in case A coupling of L and S would be the $^1\Sigma_u$. Unless this state has an extremely different value of equilibrium internuclear separation from that of the ground state, a transition to it should have already been observed in classical absorption spectra and thus, by elimination it would appear the green band should be attributed to the transition $X \rightarrow {}^1\Sigma_u$. If this is the case, then that state would have only a single value of the projection of the total angular momentum on the internuclear axis, $\Omega = 0^+$. It would be nondegenerate and would be correlated with a single dissociation limit, either $5\,^2D_{3/2}$ or $5\,^2D_{5/2}$, but not both. In that case a photolysis band in the green leading to the population of a single product state should have been obtained in contrast to the actual results shown in Fig. 6.

A satisfactory explanation of the green photolysis bands can be based upon the correlation scheme shown in Fig. 8. In this figure $^1\Sigma_u$ is assumed to be repulsive at large internuclear separation but weakly bound at smaller values. Crude estimates based upon the classical spectroscopy of Gupta *et al.*[13] have given values of $T_e = 16\,900$ cm and $r_e = 0.48$ nm for this state. Although the potential maximum implied by the long range repulsion assumed in this bound state is shown in Fig. 8, it is not necessary for the explanation following.

As shown in Fig. 8, to support this explanation the $^1\Sigma_u$ state has been assumed to be correlated with the $5\,^2D_{5/2}$ limit. It is also likely, however, that some repulsive state correlates with $5\,^2D_{3/2}$ and, if so, that state could predissociate vibrationally excited populations of $^1\Sigma_u$ lying energetically above the separated atom limit for the production of $5\,^2D_{3/2}$. Thus, for photolysis at transition energies near to the vertical excitation energy to the separated atom limits, the component of the population of the $^1\Sigma_u$ state produced with vibrational energies sufficient to place the total energy between the limits for separation into $5\,^2D_{3/2}$ and $5\,^2D_{5/2}$ products would be predissociated into $5\,^2D_{3/2}$ products. The component with vibrational energy sufficient for the total energy of the molecule to exceed the limit for separation into $5\,^2D_{5/2}$ would simply dissociate into that product channel. It would be consistent with this model to expect that with increasing transition energy, a value would be reached at which the branching ratio between products would begin to strongly favor the higher energy product with further increases in the photolysis energy. This would result when the transition energy exceeded that necessary to reach, from the minimum of the ground state potential, the separated atom limit for the dissociation into the higher energy product plus the energy needed to surmount any potential maxima in that state.

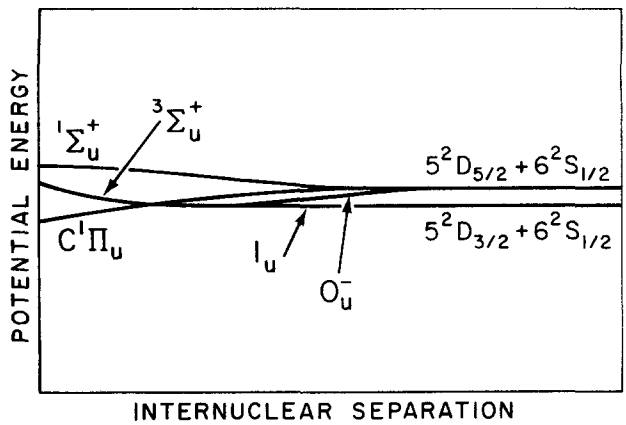

FIG. 8. Details of the correlation diagram relating the excited states of Cs_2^*, important in this experiment, to their dissociation limits.

Precisely this behavior is seen in the branching ratios plotted in Fig. 7. For energies greater than about 17 940 cm^{-1} the branching ratio increasingly favored the $5\,^2D_{5/2}$ product. Comparison to Fig. 6 shows that the decrease in the plotted ratio at transition energies greater than that of the peak in Fig. 7 may not have been statistically significant because of the small value of cross section for the production of $5\,^2D_{3/2}$ at those energies. This value of 17 940 cm^{-1} for the excitation energy necessary to reach the dissociation limit for the production of $5\,^2D_{5/2}$ atoms is consistent with a potential maximum of about 140 cm^{-1} in the $^1\Sigma_u$ state. This would be of a reasonable size but, as mentioned above, would not be necessary to explain the branching ratio data. The same behavior would result from a lowering of the energy of the initial $X\,^1\Sigma_g$ state by increasing its dissociation energy to $D_e = 3340$ cm^{-1} and would require no potential maximum. Thus, the combination of factors including the occurrence of the photolysis band in the green near the limits for separation into $5\,^2D$ atoms, the predominance of the higher energy branch to $5\,^2D_{5/2}$ and the strong increase in branching ratio at 17 940 cm^{-1} seem to indicate that the green band is the result of excitation of the $^1\Sigma_u$ state near to its dissociation limit so that both dissociation into $5\,^2D_{5/2}$ products and predissociation into $5\,^2D_{3/2}$ atoms are possible.

The blue photolysis bands shown in Fig. 6 are clearly another matter. The transition energy lies considerably above the limits for separation into the D-state products. While this might first seem to imply that the bands are simply the result of transitions, such as (1b) in Fig. 1, directly to two repulsive states that comprise different fine-structure components, each correlated with a different atomic limit, two factors argue against this interpretation. First, the electronic states correlated with $Cs(5\,^2D) + Cs$ to which allowed transitions might be made, have already been used to explain other phenomena, so that the state would have to be one normally forbidden to excitation from the ground state of Cs_2. A more serious objection is the close similarity in the appearance of these photolysis bands to the blue absorption bands of Cs_2, recently analyzed and shown[18,19] to belong to the transition, $X \rightarrow E$, between bound states.

The upper E state has been considered to be either a $^1\Sigma_u$ or a $^1\Pi_u$, and so, must correlate with a more energetic limit such as $Cs(7\,^2S)+Cs$ or $Cs(7\,^2P)+Cs$. Because of this similarity, it is more probable that predissociation of the bound E state by a repulsive state correlated with $Cs(5\,^2D)+Cs$ is the predominant mechanism for the observed photolysis. Such a system would be comparable to the case shown in Fig. 1 when excited by the (1a) transition.

The extent of the blue photolysis bands indicate that if predissociation is occurring it must be due to potential curves which almost parallel the inner limb of the bound E-state potential, so that predissociation can occur for all wavelengths normally used to excite the $X \rightarrow E$ transition. At the same time, the predissociation must be sufficiently weak to have permitted the observation of discrete structure in the bound state.[18,19] An example[44] meeting both of these conditions is the well-known predissociation of the $B\,^3\Pi$ state of I_2.

To explain the excitation of both the $J=\frac{3}{2}$ and $\frac{5}{2}$ product channels through the predissociation of the bound E state would require the proximity of a degenerate repulsive state having components correlating with both possible products. While case A coupling would require spin conservation during predissociation thereby making $^1\Delta_u$ the most likely candidate, the single fine-structure component, $\Omega=2$, of $^1\Delta_u$ would seem to preclude its possible separation into two products. This seems to imply that the appropriate coupling scheme for these highly excited states is not purely case A and that spin is not a rigorous quantum number of this heavy molecule.

Once the selection rule $\Delta S=0$ is removed from the predissociation step, all of the triplet states become equivalent candidates for the role of the repulsive state nested closely to the E state at the smaller separations inside its potential minimum. Of these, $^3\Sigma_u$ appears the most probable because of the results of the study of photolysis into $6\,^2P$ product states reported in the companion article.[14] For reasons explained there, it appears that $^3\Sigma_u$ is the most repulsive of the states in the manifold correlated with $Cs(5\,^2D)+Cs$. The correlation scheme shown in Fig. 8 is, then, sufficient to provide a basis for interpreting the occurrence of the two photolysis bands observed in the blue.

The $^3\Sigma_u$ state that is presumed to be responsible for predissociating the bound E state, has been drawn in Fig. 8 to correlate with both fine-structure components of the dissociation limit. In particular the 0_u^- component of $^3\Sigma_u$ has been correlated with the higher energy $5\,^2D_{5/2}$ limit while the degenerate 1_u components have been correlated with $5\,^2D_{3/2}$. Selection rules on the quantum number Ω allow a $^1\Pi_u$ state to predissociate to 0_u^- and both 1_u components of $^3\Sigma_u$. If it is assumed that predissociation is equally probable into each, then a branching ratio of 2 : 1 would be expected between $5\,^2D_{3/2}$ and $5\,^2D_{5/2}$, respectively. It can be seen from Fig. 7 that this agrees roughly with the branching ratio actually observed for transition energies corresponding to the blue bands.

Thus, it appears that the green photolysis bands of Cs_2 are the result of dissociation and predissociation of the $^1\Sigma_u^+$ state, while the blue bands are the result of predissociation of the bound E state by a $^3\Sigma_u$ state. As shown by the data, both cases led to identification of broad absorption bands over which reasonable product selectivity was maintained. The photolysis spectra obtained in this work clearly support the contention stated in the introductory material that relatively broadband irradiation of Cs_2 could lead to the selective population of even a single fine-structure component of the possible dissociation products. In addition to encouraging these pragmatic goals, the spectra provided a basis for the development of a better understanding of the dissociation mechanisms mediating the photolysis of Cs_2 and from that, a better understanding of the structure of the excited states of Cs_2 that are correlated with the dissociation products of interest in this work. It appears that the multiphoton technique introduced in an earlier report[12] and fully implemented here, has proven itself to be an extremely sensitive tool for the study of this type of selective photolysis of simple molecules through electronically excited states.

ACKNOWLEDGMENTS

This work was supported in part by the National Science Foundation under Grant No. INT 76-18982 under the U.S.-Romanian Cooperative Program in Atomic and Plasma Physics. In addition to the authors wish to acknowledge the invaluable assistance of Dr. Francis W. Lee of the University of Texas at Dallas. Without the contribution of his insight and expertise, this work could not have been accomplished.

[1] C. D. Cantrell, S. M. Freund, and J. L. Lyman, in *Laser Handbook* Vol. III(b), edited by M. L. Stitch (North Holland, New York, 1979), pp. 485–576.
[2] M. LuVan, G. Mainfray, C. Manus, and I. Tugov, Phys. Rev. A 7, 91 (1973).
[3] C. B. Collins, B. W. Johnson, M. Y. Mirza, D. Popescu, and I. Popescu, Phys. Rev. A 10, 813 (1974).
[4] C. B. Collins, S. M. Curry, B. W. Johnson, M. Y. Mirza, M. A. Chellehmalzadeh, J. A. Anderson, D. Popescu, and I. Popescu, Phys. Rev. A 14, 1662 (1976).
[5] N. M. Shen and S. M. Curry, Opt. Commun. 20, 392 (1977).
[6] M. Y. Mirza and W. W. Duley, Proc. R. Soc. London Ser. A 364, 255 (1978).
[7] M. Y. Mirza and W. W. Duley, Opt. Commun. 28, 179 (1979).
[8] M. McClintock and L. C. Balling, J. Quantum Spectrosc. Radiat. Transfer 9, 1209 (1969).
[9] J. E. Mentall and P. M. Guyon, J. Chem. Phys. 67, 3845 (1977).
[10] E. K. Kraulinya and M. L. Yanson, Opt. Spektrosk. 46, 1112 (1979) [Opt. Spectrosc. (USSR) 46, 629 (1979)].
[11] R. T. M. Su, J. W. Bevan, and R. R. Curl, Jr., Chem. Phys. Lett. 43, 169 (1979).
[12] C. B. Collins, J. A. Anderson, F. W. Lee, P. A. Vicharelli, D. Popescu, and I. Popescu, Phys. Rev. Lett. 44, 139 (1980).
[13] R. Gupta, W. Happer, J. Wagner, and E. Wennmyr, J. Chem. Phys. 68, 799 (1978).
[14] Part II, following paper.
[15] F. W. Loomis and P. Kusch, Phys. Rev. 46, 292 (1934).
[16] P. Kusch and M. M. Hessel, J. Mol. Spec. 25, 205 (1968).
[17] P. Kusch and M. M. Hessel, J. Mol. Spec. 32, 181 (1969).
[18] H. Kato and K. Yoshihara, J. Chem. Phys. 71, 1585 (1979).

[19]G. Honing, M. Czajkowski, M. Stock, and W. Demtroder, J. Chem. Phys. 71, 2138 (1979).
[20]D. Popescu, M. L. Pascu, C. B. Collins, B. W. Johnson, and I. Popescu, Phys. Rev. A 8, 1666 (1973).
[21]C. B. Collins, B. W. Johnson, D. Popescu, G. Musa, M. L. Pascu, and I. Popescu, Phys. Rev. A 8, 2197 (1973).
[22]D. Popescu, C. B. Collins, B. W. Johnson, and I. Popescu, Phys. Rev. A 9, 1182 (1974).
[23]M. Fabry, J. Quant. Spectrosc. Radiat. Transfer 16, 127 (1976).
[24]B. Liu and R. E. Olson, Phys. Rev. A 18, 2498 (1978).
[25]K. H. Kingdon, Phys. Rev. 21, 408 (1923).
[26]P. D. Foote and F. L. Mohler, Phys. Rev. 26, 195 (1925).
[27]F. L. Mohler, P. D. Foote, and R. L. Chenault, Phys. Rev. 27, 37 (1926).
[28]F. L. Mohler and C. Boeckner, J. Res. Natl. Bur. Stand. 5, 51 (1930).
[29]I. Popescu, C. Ghita, A. Popescu, and G. Musa, Ann. Phys. (Leipzig) 18, 103 (1966).
[30]D. Popescu, I. Popescu, J. Maurer, C. B. Collins, and B. W. Johnson, Phys. Rev. A 12, 1425 (1975).
[31]E. I. Toader, C. B. Collins, B. W. Johnson, and M. Y. Mirza, Phys. Rev. A 16, 1490 (1977).
[32]K. R. Spangenberg, *Vacuum Tubes* (McGraw-Hill, New York, 1948), Chap. 8.
[33]J. D. Cobine, *Gaseous Conductors* (Dover, New York, 1958), Chap. 6.
[34]M. A. Chellehmalzadeh and C. B. Collins, Phys. Rev. A 19, 2270 (1979).
[35]Y. T. Lee and B. H. Mahan, J. Chem. Phys. 42, 2893 (1965).
[36]M. Klewer, M. J. M. Beerlage, J. Los, and M. J. Van der Wiel, J. Phys. B 10, 2809 (1977).
[37]G. V. Marr and S. R. Wherrett, J. Phys. B 5, 1735 (1972).
[38]J. B. Taylor and I. Langmuir, Phys. Rev. 51, 753 (1937).
[39]I. Langmuir and K. H. Kingdon, Phys. Rev. 21, 380 (1923).
[40]I. Langmuir and K. H. Kingdon, Proc. R. Soc. London, Ser. A 107, 61 (1925).
[41]S. Dushman, Rev. Mod. Phys. 2, 381 (1930).
[42]K. Spangenberg, *Vacuum Tubes* (McGraw-Hill, New York, 1948), Chap. 4.
[43]O. S. Heavens, J. Opt. Soc. Am. 51, 1058 (1961).
[44]For a review of the predissociation of I_2, see: R. S. Mulliken, J. Chem. Phys. 55, 288 (1971).